

Supercoiled DNA is interwound in liquid crystalline solutions

Jim Torbet and Elisabeth DiCapua

Institut Laue-Langevin, 156 X, 38042 Grenoble Cedex, France

Communicated by D.M.J.Lilley

Two structures have been proposed for supercoiled DNA: it is idealized either as a toroidal ring or as a rod of two interwound duplex chains. The latter model is the most widely depicted but the evidence remains controversial. We have worked with monomers and dimers of two plasmids, pUC8 and pKS414, of similar size and natural superhelical density. pKS414 contains a bend promoting sequence whereas pUC8 does not. In concentrated solutions these plasmids form a partially ordered liquid crystalline phase which is found, using neutron diffraction, to consist of a hexagonally packed assembly of parallel rod-like particles. This shape strongly suggests an interwound conformation for which some structural parameters are deduced. The mass/unit length obtained by combining the area of the hexagonal lattice and the concentration is ~ 3.6 times that of linear DNA. This implies a shallow superhelical pitch angle $\sim 36^\circ$ which, when combined with the known number of supercoil turns, yields the pitch ~ 360 Å and radius ~ 80 Å for the supercoil. Oriented X-ray fibre diffraction patterns at 92% relative humidity indicate a B type duplex structure. Nicked circular plasmids also form liquid crystals but their behaviour, as a function of concentration, differs from that of the superhelical plasmids.

Key words: DNA structure/liquid crystals/supercoil structure

Introduction

Most DNA is negatively supercoiled *in vivo* and supercoiling plays a role in a number of important cellular events (e.g. gene expression, replication and recombination). The conformation of this DNA will depend very much on its interaction with protein to which most of it is complexed. Equally the DNA conformation might have a considerable effect on cellular events by influencing the sites of protein attachment, the translocation of bound protein or interactions involving distant sites on the DNA. It is therefore of prime importance to find out as much as possible about the architecture of superhelical DNA and how it can be influenced, e.g. by bend inducing sequences which have been located in the origin of replication (Ryder *et al.*, 1986; Stenzel *et al.*, 1987; Zahn and Blattner, 1987) and found to favour nucleosome formation (Hsieh and Griffith, 1988). The concentration of DNA *in vivo* can range up to ~ 700 mg/ml as in sperm heads, bacterial nucleoids and virus cores. In some cases liquid crystalline properties are observed (Livolant, 1984). Thus the investigation of the behaviour of purified DNA, particularly when superhelical, at high

concentrations might provide information about the packing mechanisms involved.

A number of physico-chemical techniques have been employed in order to elucidate the structure of superhelical DNA in solution. Low angle X-ray scattering has been interpreted as showing the existence both of toroidal (Brady *et al.*, 1976) and interwound structures (Benham *et al.*, 1980; Brady *et al.*, 1983), although these authors have now concluded that the former predominates (Brady *et al.*, 1987). However, this proposal is at odds with electron microscopy which usually gives images that are consistent with an interwound conformation (e.g. Bourguignon and Bourgaux, 1968; Rhoades and Thomas, 1968; Laundon and Griffith, 1988). Although the intervention of preparative and spreading procedures could give rise to artifacts it would be surprising if they simply induced a switch from a toroidal to a predominantly interwound form. Also the interpretation of the solution X-ray scattering curves is not straightforward as they are of low resolution and rather featureless, so that a good fit between measured and calculated curves is by no means conclusive proof of the validity of a model. Sedimentation (Gray, 1967; Bottger and Kuhn, 1971) and light scattering (Campbell, 1978) measurements suggest that the conformation depends on the solution conditions. By using recombination to probe the DNA structure it has been shown that the interwound supercoil exists both *in vitro* (Spengler *et al.*, 1985; Bliska and Cozzarelli, 1987) and *in vivo* (Bliska and Cozzarelli, 1987).

As short fragments of linear duplex DNA form liquid crystalline phases that are susceptible to magnetic orientation (Brandes and Kearns, 1986; Senechal *et al.*, 1980; Strzelecka *et al.*, 1988), we decided to look for similar properties in solutions of superhelical plasmids. The work was performed on monomers and dimers of pUC8 and pKS414, the monomers of which have 2717 and 2671 bp respectively. All had a superhelical density of about -0.05 . The main difference between these plasmids is that pKS414 contains a bend inducing sequence of 150 bp derived from a kinetoplast DNA minicircle (Diekmann and Wang, 1985) and its dimer has two such sequences maximally separated on the DNA circle.

Results

Superhelical plasmids form liquid crystals

Above ~ 45 mg/ml up to the highest concentration studied (~ 80 mg/ml), the translucent solutions are seen to be composed of birefringent domains, typical of liquid crystals, when viewed between crossed-polarizers. At lower concentrations down to ~ 30 mg/ml the solutions remain translucent and weakly birefringent. The neutron diffraction patterns from samples with concentrations above ~ 45 mg/ml display a symmetrical pair of peaks at Bragg spacings d and $d/\sqrt{3}$ (Figure 1), reflecting a two-dimensional hexagonal lattice,

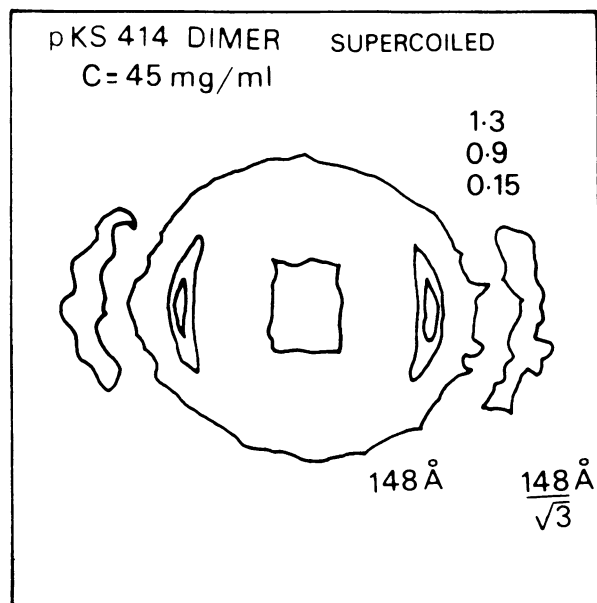


Fig. 1. An example of the neutron diffraction pattern obtained at room temperature from a solution of the superhelical dimer of pKS414 at a concentration of 45 mg/ml (D_2O with 10 mM Tris-HCl, 0.5 mM EDTA; pH = 7.4). The heights of the contour lines are indicated. Samples were frequently found to be spontaneously oriented as shown here. Also orientation could be deliberately induced by shearing the solutions in a bench centrifuge.

which immediately suggests parallel rod-like particles. Furthermore, the Bragg spacings plotted against the reciprocal of the square root of the concentration lie, within experimental error, on straight lines that pass through the origin (Figure 2). This two-dimensional behaviour means that the rods move apart only laterally as dilution proceeds. A rod-like structure which is relatively uninfluenced by end effects is also supported by the near identity of the slopes obtained from monomers and dimers (Figure 2). Finally, the good linearity of the plots through the origin (Figure 2) shows that the solutions contain one phase and that the molecular shape is rather constant over the concentration range investigated (Bernal and Fankuchen, 1941; Luzzati *et al.*, 1961). Thus the behaviour of these solutions is typical of liquid crystalline solutions of rod-like polyelectrolytes such as TMV (Bernal and Fankuchen, 1941), linear duplex DNA at high concentrations (Luzzati *et al.*, 1961) and filamentous bacteriophages Pf1 and fd (J.Torbet and G.Maret, unpublished data). Hence we conclude that superhelical plasmids are rod-like and thus have an interwound conformation at least when constrained in a liquid crystalline state. At the end of the following section after having discussed the structure of the interwound molecule and presenting additional data on magnetic orientability we argue further that the structure is unlikely to be toroidal.

All four plasmids display the same behaviour, which implies that the sequence directed bends either do not significantly disrupt the superhelical structure by, for example, introducing branching, or are preferentially situated at the looped ends. If the bend promoting sequences are located in the latter position then one would expect the behaviour of a trimer of pKS414 to differ from that found above because such a molecule could not be rod-like, as it would have three looped ends and therefore be branched. In preliminary measurements, in collaboration with

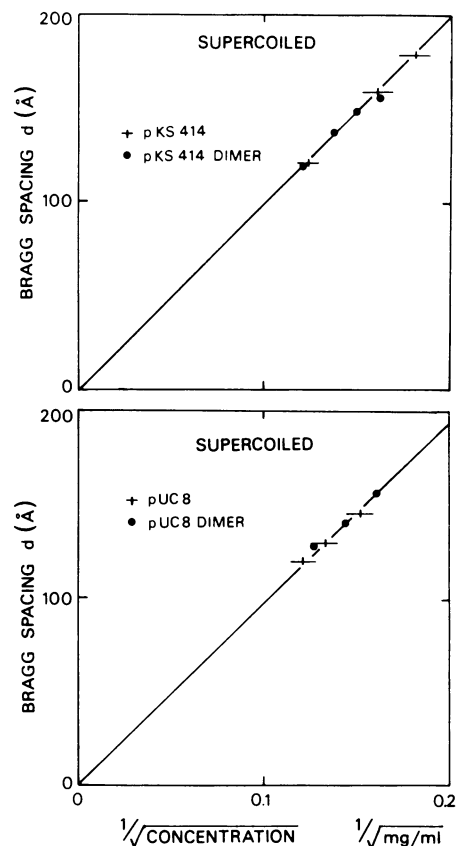


Fig. 2. Plot of the first order Bragg spacing d , from neutron diffraction (e.g. Figure 1) as a function of the reciprocal of the square root of the concentration for monomers and dimers of pKS414 and pUC8. The intensity of the reflections diminishes with decreasing concentration so that with the same measuring time no maxima were observed below ~ 30 mg/ml. The straight lines are fitted through the origin, otherwise the intercept of the pUC8 data is displaced to $d = 16$ Å and the slope is slightly reduced. A small positive d intercept is not surprising as up to 10% nicked material is present.

U.Giesen, we have indeed found that for such a plasmid, with the same superhelical density as used here, the variation of the Bragg spacing with concentration differs significantly from that observed for the monomers and dimers reported in Figure 1. Recent electron microscopy (Laundon and Griffith, 1988) is consistent with the preferential positioning of bend favouring sequences at the ends of an interwound structure.

Structural parameters of supercoils in liquid crystals

The volume (\AA^3) available per molecule of mol. wt M at concentration C (g/ml), is $10^{24} * M / CN_A$ ($N_A =$ Avogadro's number). The volume occupied by rods of axial length L , packed parallel into a hexagonal lattice, is $Ld^2 * 2/\sqrt{3}$ (d is the first order Bragg spacing) provided the gaps at the ends are small. Then by division the average mass per unit length, M/L , is given by $10^{-24} * N_A C d^2 * 2/\sqrt{3}$. Using the slope of the straight lines in Figure 2, and reducing C by 5% to take some account of the concentration of nicked plasmid, we calculate $M/L = 650 \pm 70$ daltons/Å for all four plasmids.

The superhelical pitch angle, β , is calculated to be $36 \pm 5^\circ$ from the relation $\sin\beta = 2*190/650$ (that is twice the mass per unit length of linear B form DNA, as the interwound structure has an up and down chain, divided by the value of M/L reported above). This low value for β is

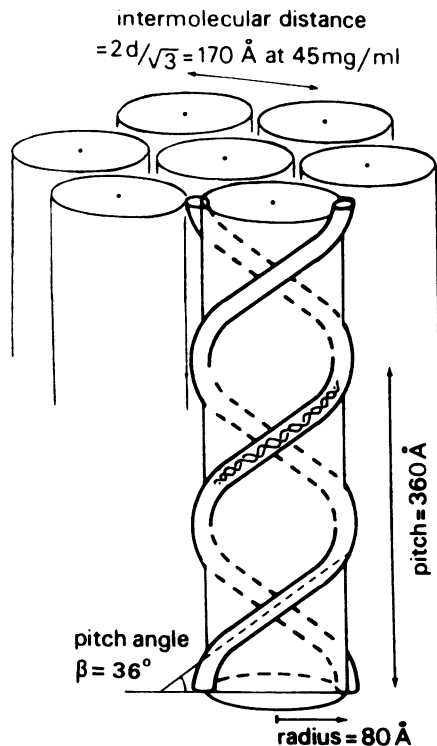


Fig. 3. Sketch of the superhelix showing the parameters we have derived. The packing dimensions are also shown for a concentration of 45 mg/ml as in Figure 1.

corroborated by the magnetic orientation behaviour discussed below.

The approach adopted here is copied from early X-ray work (Luzzati *et al.*, 1961) on liquid crystals of linear duplex DNA. On that occasion the estimate of the mass per unit length confirmed the presence of B form DNA in solution and hence demonstrates the validity of the method.

Knowledge of the number of superhelical turns is not required for the determination of β ; however, it is necessary for the determination of the contour length, l , of one superhelix turn. Once the values of β and l are known then the average pitch, p , and radius, r , of the interwound superhelix can be deduced from the following relationships, $p = l \sin \beta$ and $2\pi r = l \cos \beta$. We assume the number of supercoils in the liquid crystalline state to be about the same as that observed in electrophoresis. Support for this assumption is drawn from electron microscopy which has shown that the number of supertwists seen corresponds to the values obtained from gels (Sperrazza *et al.*, 1984). We thus calculate $l = 630 \pm 30 \text{ \AA}$ (i.e. $2700 \text{ bp} \times 3.5 \text{ \AA}/14.5$ turns) which results in a pitch and radius of $360 \pm 40 \text{ \AA}$ and $80 \pm 8 \text{ \AA}$ respectively. A large solvent filled core equivalent in width to about six duplex diameters is surrounded by a very open helical filament (Figure 3). This very open structure occupies a large volume relative to its mass and indeed above $\sim 45 \text{ mg/ml}$ the volumes occupied by adjacent molecules must overlap. From the preceding equations it is evident that if the number of superhelical turns is smaller or larger than that estimated by electrophoresis then both p and r will increase or decrease in proportion.

In liquid crystals of short fragments of linear duplex DNA (Senechal *et al.*, 1980) the molecules orient with their long axis perpendicular to the direction of a strong magnetic field. We have also observed this behaviour with liquid crystalline

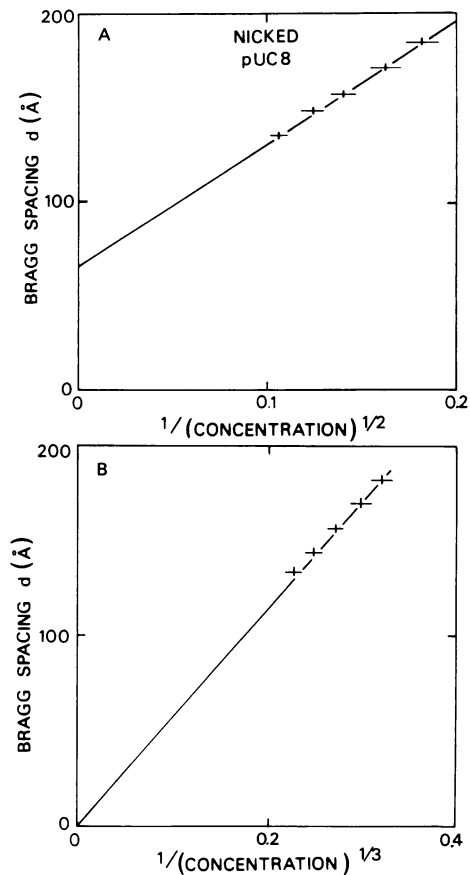


Fig. 4. Plot of the first order Bragg spacing d obtained by neutron diffraction from nicked circular pUC8 monomer, as a function of the reciprocal of (A) the square root and (B) the cubed root of the concentration measured in mg/ml. Nicked plasmids also give liquid crystalline solutions that give two Bragg orders at d and $d/\sqrt{3}$ (as in Figure 1) reflecting a hexagonal lattice. The sample contained $<5\%$ superhelical plasmid.

phases of nicked circular plasmids in fields of 60 kGauss. Orientation is due to the diamagnetic anisotropy of the molecules which comes predominantly from the bases whose minimum energy orientation is with their planes parallel to the magnetic field. In contrast, even after being left standing for several days at room temperature in 60 kGauss field, produced by a superconducting magnet, superhelical samples showed little sign of magnetically induced orientation. This suggests that the molecular conformation is such as to give rise to a zero or weak diamagnetic anisotropy. As the diamagnetic anisotropy comes largely from the bases then the axis of the double helix must follow a trajectory such that the anisotropy of the bases averages out. The diamagnetic anisotropy of the superhelix axis is proportional to the orientation factor, $1.5 \sin^2 \beta - 0.5$, as derived by Maestre and Kilksen (1965). Thus a small diamagnetic anisotropy implies that $\beta \approx 35^\circ$.

Another structure that could conceivably give rise to the diffraction observed is that of a toroid distorted by the liquid crystal packing forces into two parallel helical rods linked by short loops. If these rods occupy a hexagonal lattice then $\sin \beta$ is now equal to $(190/650)$, half the value obtained for the interwound structure, because there is now only half a molecule per unit cell. Hence $\beta = 16^\circ$ and r and p , calculated as above, are respectively 96 and 175 Å. However it is doubtful that the dilution behaviour of such a structure

would be as simple as that observed (Figure 2) because this would require the distance between the covalently linked and adjacent rods to remain equal at all concentrations. Indeed the behaviour of distorted toroids is more likely to resemble that for nicked plasmids reported below (Figure 4). Furthermore for such a low pitch angle, orientation parallel to the magnetic field direction would be expected. Our data are much more consistent with an interwound conformation.

Nicked plasmids also form liquid crystals

Solutions of nicked circular plasmids also give hexagonal Bragg diffraction similar to that shown in Figure 1, again indicating a hexagonal arrangement of rods. Deformation of the molecular shape away from that found in free solution into a much more elongated or rod-like conformation is probably both a prerequisite for and a consequence of liquid crystal formation. Thus ring-like molecules that are neither inherently rod-like or in a fixed conformation can form liquid crystals. The variation of d with $1/\sqrt{C}$ is linear (Figure 4) but the slope is less than half that of the superhelical plasmids (Figure 2) and the intercept on the d axis (65 Å) is displaced far above zero. The apparent M/L decreases from 1100 at the highest to 700 daltons/Å at the lowest concentration. Thus the nicked and superhelical plasmids behave in fundamentally different ways.

The increase in the apparent M/L of the nicked plasmid with increasing concentration (Figure 4) could be because the fraction of the DNA in the liquid crystalline phase decreases and/or because the molecules become more compact (i.e. shorter). As the liquid crystalline packing forces increase with concentration neither of these explanations appears to be physically plausible. The most coherent explanation of these results we have been able to formulate is as follows. The nicked circular molecules are in the form of two parallel duplex chains with relatively short end loops ($M/L \approx 2 \times 190$ daltons/Å). Because the two chains in any one molecule are covalently continuous they are subject to additional constraints so that the distance between them differs from that to the chains of adjacent molecules. Three of these molecules pack into the hexagonal unit cell giving an M/L close to that found at the highest concentration. Now when the data are plotted against $C^{-1/3}$ the extrapolated straight line passes close to the origin, which suggests that the total length of the unit cell changes along with and approximately in proportion to the Bragg spacing of the hexagonal lattice. Thus the nicked molecules not only increase their lateral separation upon dilution, in the manner found when they are superhelical, but their end to end separation also increases and gives rise to an apparent reduction in the M/L . This is possibly because there is a tendency for the molecular shape to change (i.e. open up) which is, however, restrained by the forces arising from neighbouring molecules which also have two chains trying to swell apart. These results are not without biological interest as relaxed circular DNA occurs in, for example, cauliflower mosaic virus (Hull and Shepherd, 1977).

X-ray fibre diffraction from superhelical plasmids

We have carried out some exploratory experiments in order to find out if X-ray fibre diffraction could contribute to the study of superhelical structure. Fibres were made in the classical way by slowly drying a small volume of solution suspended between the tips of fine glass rods. When X-rayed

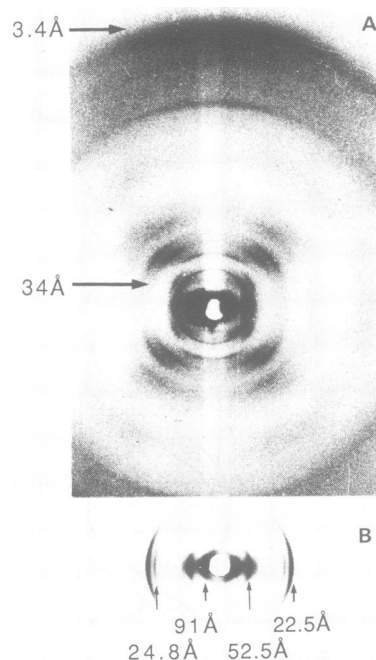


Fig. 5. X-ray diffraction from a fibre of the dimer of pUC8 in an atmosphere of 92% relative humidity. (A) The high angle pattern resembles that from relaxed B type DNA. The specimen to film distance was 5.47 cm. The vertical shadow is due to absorption in the sealed glass capillary tube used to hold the fibre. The first (34 Å) and (3.4 Å) tenth layer lines are indicated. (B) The specimen to film distance was increased to 10.5 cm. The prominent equatorial reflections are indicated. There is a reflection at 45.5 Å forming a weak shoulder on the strong 52.5 Å peak. A very weak diffuse reflection at 36 Å is not visible on the reproduction. All these reflections save the latter can be indexed on a two-dimensional hexagonal lattice as follows: 91 Å (10), 52.5 Å (11), 45.5 Å (20), 24.8 Å (31), 22.5 Å (40).

at 92% relative humidity, these samples showed no low angle diffraction from the superhelix but at higher angles a crossed helical diffraction pattern is recorded with the layer lines spaced by 34 Å and a strong meridional at 3.4 Å (Figure 5A). The general form of the pattern is that of B type DNA which is a regular helix with 10 bp in a helix of ~ 34 Å pitch. However, in Figure 5 the 8th layer line peaks on or near the meridian and the weak first layer line is a rather uniform streak of intensity crossing the meridian. The selection rules for helical diffraction exclude meridional reflections from a regular 10-fold helix save on the 10th layer line. Thus the duplex structure of superhelical DNA is perturbed in these conditions.

The equatorial reflections can be indexed on a hexagonal lattice with a unit cell dimension of 105 Å (i.e. $91 \times 2/\sqrt{3}$) save for a very weak reflection around 36 Å, which may be due to the presence of nicked plasmid. If the molecules are not able to interpenetrate, 105 Å would be close to the maximum possible outer diameter. However, the diameter of the interwound superhelices may be larger because they must have large surface grooves which could easily accommodate duplexes from adjacent molecules. (A degree of interlocking or interpenetration already occurs in the liquid crystalline phase studied above.) But as the estimated diameter (≈ 160 Å) in liquid crystals is significantly larger it is probable that a transition to a thinner more elongated form has occurred in the fibre. Indeed this conclusion is

supported by the high angle diffraction (Figure 5A) which is so like that from linear DNA that it suggests a steep pitch angle for the superhelix. Nevertheless even in these relatively dehydrated fibres the structure must have an open solvent filled core as an interwound helix with touching chains would have a total width of the order of only two duplex diameters (i.e. $\approx 40 \text{ \AA}$).

All sorts of conformational changes might inevitably occur during fibre formation. The close proximity of the molecules, the dehydration concomitant with the concentration of salt must result in changes in the packing forces. The open highly hydrated conformation (Figure 3) may very well become thinner as discussed above and the regularity of the superhelical structure might be diminished, or indeed improved, by intermolecular interactions. Also the number of superhelical turns might be altered due to the increase in salt concentration (Anderson and Bauer, 1978) or the influence of some other variable. Therefore fibre diffraction is unlikely to have the same success with superhelical DNA as it has had with the linear duplex form. Nevertheless it may have some uses, e.g. it could reveal if the salt and hydration dependent polymorphism documented in the linear molecule (e.g. Arnott *et al.*, 1983) also occurs under torsional stress. The evolution in the high angle diffraction pattern, as oriented fibres are slowly hydrated towards dissolution, might give more information about superhelical structure than simply working with dehydrated fibres and shear oriented liquid crystals.

Discussion

We have shown that superhelical DNA with a negative superhelical density of about -0.05 takes up an invariant interwound conformation in liquid crystals at concentrations ranging from 30 to 90 mg/ml. The mass per unit length, pitch and diameter of the structure have been derived (summarized in Figure 3). There is no evidence for a toroidal structure at these superhelical densities but we cannot exclude the presence of this form in dilute solution when the forces associated with liquid crystallinity are absent. However, there are very few data in favour of a toroidal structure and the most prominent evidence comes from X-ray solution scattering (Brady *et al.*, 1976, 1987) which, as we have already discussed in the Introduction, must be interpreted with caution.

In partly dehydrated fibres the interwound structure is probably stretched to form a helix with a larger pitch and smaller diameter but retains a large solvent filled core separating the up and down chains. Nicked plasmids also form liquid crystals over the same concentration range but their conformation is concentration dependent. It would be of interest to find out if this change, from an invariant to a varying structure, is gradual or is more or less localized in superhelical density. Of particular interest is the behaviour of plasmids with a superhelical density similar to the average value of -0.024 estimated for unconstrained cellular DNA (Bliska and Cozzarelli, 1987).

The question of superhelical structural regularity remains a moot point. Our attempts to observe the superhelical pitch directly in the liquid crystalline phase using neutron diffraction and in partly dehydrated fibres with X-ray diffraction were unsuccessful. This may be because the structure is loose and without a well defined pitch. On the

other hand, our samples are not monodisperse as they contain a number of topoisomers each with a different structure. Better results might be obtained by using samples with a smaller distribution in the number of superhelical turns and plasmids with sequences which might promote a more regular superhelical structure. But it should be borne in mind that the sharp B type diffraction pattern from fibres of linear duplex DNA becomes increasingly more diffuse as the water content is increased (Zimmerman and Pfeiffer, 1979). So as there are far fewer supercoils than duplex turns with, most probably, a lesser degree of regularity, it is not surprising that the superhelical pitch does not show up in diffraction patterns at high degrees of hydration. As oriented samples can be obtained from both superhelical and nicked plasmids in similar conditions their comparison might lead to a better understanding of the effect of supercoiling on the duplex structure.

There are considerable differences between the conditions of our experiments and those prevailing in the cell. It has been estimated that some 60% of the supercoils are constrained by interactions with protein and other cellular components (Bliska and Cozzarelli, 1987). Supercoils are thus partitioned into bound and free regions. During transcription a gradient of both negative and positive supercoils is found on opposite sides of the RNA polymerase (Wu *et al.*, 1988). Thus the free supercoils belong to a family of topological domains each with different properties depending on their size, superhelical density (positive and negative) and features of their nucleotide sequence. Different domain conformations might well influence gene expression to different degrees.

One way of gaining some insight into the topology of free supercoiled DNA is by studying the behaviour of purified plasmids of different size, sequence and superhelical density. Thus the nicked and superhelical plasmids studied here model the behaviour of domains with low and intermediate superhelical densities respectively. Our nicked plasmids are deformed into a highly elongated shape when liquid crystalline, which suggests that the domains of relaxed DNA have a rather variable tertiary conformation that can be strongly influenced by environmental forces. In contrast the liquid crystalline superhelical plasmids have an invariant interwound structure. Hence by extrapolation, cellular domains of intermediate superhelical density adopt a rather stable interwound structure. As the diameter of the proposed structure (Figure 3) is large, the translocation of bound protein is less likely to be obstructed by the opposing chain, yet the chains are not held so far apart as to prevent cross chain protein-protein interactions.

If at intermediate superhelical densities, bend inducing sequences are indeed preferentially located at extremities of an interwound structure (the effect is likely to be diluted out as the superhelical density is decreased) then their presence in a topological domain of free DNA might have some influence on the structure of the domain by defining the probable position of the loops and so promoting a unique relationship between the sequences in each duplex strand of the interwound segment.

Materials and methods

Sample preparation

Plasmids were isolated in a cleared lysate with triton followed by deproteination with phenol. The final purification step was sedimentation

through sucrose gradients which also separated the nicked and supercoiled forms. The DNA was concentrated by ethanol precipitation from 0.3 M sodium acetate. The pellet was washed with 70% ethanol in H₂O in order to remove excess salt. After drying in vacuum, it was transferred to a quartz cell (0.1 cm optical path length by 0.4 cm wide), weighed, and left to dissolve in buffer for at least 1 day. In order to control the dilution, a measured volume ($\approx 20 \mu\text{l}$) of D₂O buffer was added to the dry pellets (see Figure 1 legend) to give an initial concentration of $\sim 80 \text{ mg/ml}$. Dilution was then carried out in steps following each neutron measurement. All steps were monitored by accurate weighing. Solutions were usually mixed with a syringe needle, and left to equilibrate for at least 12 h before collecting the next diffraction pattern. At the end of the series of neutron experiments the concentration was determined by diluting a precise aliquot and measuring its absorbance ($E_{260}^{1\%} = 200$). The buffer was usually 10 mM Tris-HCl, 0.5 mM EDTA; pH = 7.4. Some measurements were also made at 2 and 25 mM Tris-HCl without a noticeable difference in the diffraction.

The sodium concentration in the sample is assumed to be the same as that of the DNA phosphates, i.e. $\sim 100 \text{ mM}$ at a DNA concentration of 32 mg/ml. We added a small volume of concentrated NaCl solution to add 100 mM NaCl to the total salt concentration in one sample of pUC8 at a concentration of 60 mg/ml and found that the neutron Bragg peak became broader but did not change position.

The superhelical densities of the four plasmids were determined by band counting after agarose gel electrophoresis (Keller, 1975; Shure and Vinograd, 1976). The Gaussian distribution of topoisomers spanned about six species and had a maximum between 14 and 15 superhelical turns for a plasmid of 2700 bp. In addition to this heterogeneity, the samples contained between 5 and 10% nicked circular DNA. During the neutron experiments no further nicking took place (neutrons cause much less chemical damage than X-rays).

Neutron measurements

The neutron diffraction measurements were made on the low angle scattering instrument D11 (Ibel, 1976) at the Institut Laue-Langevin which has a two-dimensional ($64 \times 64 \text{ cm}^2$) detector. A number of specimen to detector distances between 2 and 10 m were used and the wavelength was 10 Å ($\Delta\lambda/\lambda = 8\%$ full width, half maximum). The spectra showing diffraction as in Figure 1 took ~ 15 min to measure.

X-ray fibre diffraction

A few microlitres of solution 10–20 mg/ml were suspended between small glass rods and allowed to dry slowly. These fibres were equilibrated at the desired relative humidity then sealed in thin walled glass capillary tubes accompanied by, but not in contact with, some of the saturated salt solutions used to control the relative humidity. The X-ray diffraction patterns were collected using a point focused Frank's camera on an Eliot rotating anode generator JX20 at the EMBL outstation in Grenoble. The specimen to detector distance was measured using a ruler and some exposures at short specimen to film distances were calibrated using calcite which gives a ring at 3.03 Å. Various specimen to film distances between 5 and 43 cm were used.

Acknowledgements

We are grateful to S. Diekmann for supplying pKS414, to U. Giesen and C. Berthet-Colominas for help with sample preparation and X-ray diffraction respectively. We thank P. Timmins and R. May for their help with D11 and D. Hukins for commenting on the manuscript. Liquid crystalline behaviour was first observed in a sample prepared by J. Langowski. We thank the European Molecular Biology Organization for supporting E. DiCapua with a long term fellowship.

References

- Anderson, P. and Bauer, W. (1978) *Biochemistry*, **17**, 594–601.
 Arnott, S., Chandrasekaran, R., Banerjee, A. K., Rungen He and Walker, J. K. (1983) *J. Biomol. Struct. Dyn.*, **1**, 437–452.
 Benham, C. J., Brady, G. W. and Fein, D. B. (1980) *Biophys. J.*, **29**, 351–366.
 Bernal, J. D. and Fankuchen, I. (1941) *J. Gen. Physiol.*, **25**, 111–165.
 Bliska, J. B. and Cozzarelli, N. R. (1987) *J. Mol. Biol.*, **194**, 205–218.
 Bottger, M. and Kuhn, W. (1971) *Biochim. Biophys. Acta*, **254**, 407–411.
 Bourguignon, M.-F. and Bourgaux, P. (1968) *Biochim. Biophys. Acta*, **169**, 476–487.
 Brady, G. W., Fein, D. B. and Brumberger, H. (1976) *Nature*, **264**, 231–234.
 Brady, G. W., Fein, D. B., Lambertson, H., Grassian, V., Foos, D. and Benham, C. J. (1983) *Proc. Natl. Acad. Sci. USA*, **80**, 741–744.

- Brady, G. W., Foos, D. and Benham, C. J. (1984) *Biopolymers*, **23**, 2963–2966.
 Brady, G. W., Satkowski, M., Foos, D. and Benham, C. J. (1987) *J. Mol. Biol.*, **195**, 185–191.
 Brandes, R. and Kearns, D. R. (1986) *Biochemistry*, **25**, 5890–5895.
 Campbell, A. M. (1978) *Biochem. J.*, **171**, 281–283.
 Diekmann, S. and Wang, J. C. (1985) *J. Mol. Biol.*, **186**, 1–11.
 Gray, H. B. (1967) *Biopolymers*, **5**, 1009–1019.
 Hsieh, C.-H. and Griffith, J. D. (1988) *Cell*, **52**, 535–544.
 Hull, R. and Shepherd, R. J. (1977) *Virology*, **79**, 216–230.
 Ibel, K. (1976) *J. Appl. Crystallogr.*, **9**, 296–309.
 Keller, W. (1975) *Proc. Natl. Acad. Sci. USA*, **72**, 4876–4880.
 Laundon, C. H. and Griffith, J. D. (1988) *Cell*, **52**, 545–549.
 Livolant, F. (1984) *Eur. J. Cell Biol.*, **33**, 300–311.
 Luzzati, V., Nicolaieff, A. and Masson, F. (1961) *J. Mol. Biol.*, **3**, 185–201.
 Maestre, M. F. and Kilkson, R. (1965) *Biophys. J.*, **5**, 275–287.
 Rhoades, M. and Thomas, C. A. (1968) *J. Mol. Biol.*, **37**, 41–61.
 Ryder, K., Silver, S., DeLucia, A. L., Fanning, E. and Tegtmeier, P. (1986) *Cell*, **44**, 719–725.
 Senechal, E., Maret, G. and Dransfeld, K. (1980) *Int. J. Biol. Macromol.*, **2**, 256–262.
 Shure, M. and Vinograd, J. (1976) *Cell*, **8**, 215–226.
 Spengler, S. J., Stasiak, A. and Cozzarelli, N. R. (1985) *Cell*, **42**, 325–334.
 Sperrazza, J. M., Register, J. C., III and Griffith, J. (1984) *Gene*, **31**, 17–22.
 Stenzel, T. T., Patel, P. and Bastia, D. (1987) *Cell*, **49**, 709–717.
 Strzelecka, T. E., Davidson, M. W. and Rill, R. L. (1988) *Nature*, **331**, 457–460.
 Wu, H. Y., Shyy, S., Wang, J. C. and Liu, L. F. (1988) *Cell*, **53**, 433–440.
 Zahn, K. and Blattner, R. F. (1987) *Science*, **236**, 416–422.
 Zimmerman, S. T. and Pfeiffer, B. H. (1979) *Proc. Natl. Acad. Sci. USA*, **76**, 2703–2707.

Received on July 25, 1989; revised on September 11, 1989